A classical path to unification

To cite this article: K Hasselmann 2013 *J. Phys.: Conf. Ser.* **437** 012023

View the article online for updates and enhancements.

A classical path to unification

K Hasselmann

Max Planck Institute for Meteorololgy, Hamburg

E-mail: `klaus.hasselmann@zmaw.de`

Abstract. An overview is given of a classical unified theory of gravity, elementary particles and quantum phenomena based on soliton solutions of Einstein's vacuum equations in twelve dimensional space. Bell's theorem on the Einstein-Podolsky-Rosen experiment, which is widely interpreted as ruling out classical explanations of quantum phenomena, is shown to be non-applicable as violating time-reversal symmetry. Entanglement is a relativistic consequence of Newon's third law and a property of all time-symmetrical theories, whether classical or quantal. The *metr*ic solit*ons* (*metrons*) are composed of strongly nonlinear periodic core components, far fields corresponding to the classical gravitational and electromagnetic far fields of point-like particles, and further fields representing the weak and strong interactions. The core fields represent nonlinear eigenmodes trapped in a self-generated wave guide. Computations are presented for the first family of elementary particles corresponding to the lowest nonlinear eigenmodes; the second and third families are assumed to correspond to higher eigenmodes. It is shown that the periodicities of the soliton core modes produce the wave-particle duality paradoxes of quantum phenomena, as exemplified by single- and double-slit particle diffraction and the discrete structure of atomic spectra.

1. Introduction

The paradoxes faced by physicists in the beginning of the last century gave rise to two conceptual revolutions which resulted in two very different pictures of physical reality. The alternative views have still not been reconciled within a unified theory to this day.

The paradox of the Galilean invariance of the speed of light was resolved by Einstein (and later extended to arbitrary coordinate transformations) by the recognition that the concepts of space and time could not be accepted as given *a priori*, but must be defined explicitly, together with the properties of the other physical objects with which they were to be combined in a physical theory. In contrast, the paradox of the observation of both wave-like and corpuscular properties in the same microphysical phenomena was resolved by Born, Heisenberg, Jordan, Bohr, Pauli and other proponents of the new quantum theory by the opposite approach of rejecting the concept of real existing microphysical objects as meaningless. Meaningful was only the prediction of the outcome of experiments. The experiments themselves must nonetheless still be described in terms of the microphysical objects which have been declared before to defy definition.

Despite the unresolved conceptual problems of the underlying tenets of quantum theory, the theory has been extremely successful in describing a wide spectrum of quantum phenomena, many with impressive accuracy. And it has withstood for more than eight decades all attempts to demonstrate logical inconsistencies in its axiomatic structure. Indeed, the critical analysis of

Einstein, Poldolsky and Rosen [16], suggesting that quantum theory was incomplete, is widely interpreted today, in conjunction with the experimental validation of Bell's [5] inequality theorem on the EPR experiment, as demonstration that classical theories are fundamentally unable to explain the quantum theoretical phenomenon of entanglement, as exemplified by the EPR experiment.

It is therefore understandable that most unification approaches, such as string theory [22],[39] or quantum loop gravity [42],[7], seek to incorporate gravity in a broader theory that accepts the basic tenets of quantum theory, and its relativistic generalization, quantum field theory. We explore nevertheless the alternative route of generalizing Einstein's theory of gravity in order to incorporate quantum phenomena. The motivation for our approach is threefold.

First, we show in the next section that the popular "no go" misnomer [49] of Bell's theorem ignores the essential locality condition that Bell himself stressed. Entanglement is found to be a fundamental property not only of quantum theory, but of all theories, whether quantal or classical, that satisfy microphysical time-reversal symmetry. Entanglement is a necessary relativistic consequence of Newton's third law *actio = reactio*.

Secondly, we present in Section 3 a classical theory of elementary particles that resolves the wave-particle duality paradox that was the original motivation for the creation of quantum theory. Fields and particles are derived as integral components of a single object, the *metric soliton (metron)* solutions of Einstein's vaccuum equations

$$E_{LM} = 0 \tag{1}$$

in twelve-dimensional space, where

$$E_{LM} = R_{LM} - \frac{1}{2} g_{LM} R_N^N \tag{2}$$

is the Einstein tensor and R_{LM} the Ricci curvature tensor (cf. [37]; details will be given later).

The soliton solutions of eq.(1) consist of a strongly nonlinear periodic eigenmode concentrated in the soliton core, far fields corresponding to the classical electromagnetic and gravitational fields of point-like particles, and further fields representing the weak and strong forces. The solutions reproduce the basic symmetries and other properties of elementary particles.

Thirdly, we show in the Section 4 that the metron model yields a straightforward explanation of the wave-like interference properties of particles observed in microphysical phenomena. The interferences arise through the interactions of the periodic core mode of the soliton solution with its own field, after the field has been scattered off other matter. As examples, we compute the diffraction of a stream of particles for the standard single and double-slit experiments and summarize the metron interpretation of atomic spectra as an amalgam of quantum electrodynamics and the original Bohr model of orbiting electrons.

Concepts related to the metron model have been proposed previously. The interpretation of particles as solitons was popular at the turn of the 19th century (see, for example, [1], or Lorentz's [35], [36] well-known model of the electron). The advent of quantum theory, however, in response to the mounting paradoxes of microphysics, deflated the belief that particles could be represented by something as simple as solitons, and interest in this approach faded. The attribution of the wave-like interference properties of particles to a guiding periodic field was proposed by de Broglie [12],[13] and developed further by Bohm [6] (see also Holland [29]). However, in contrast to the de Brogle-Bohm "pilot" wave, which was introduced *ad hoc* as an additional external field independent of the particles (which were also prescribed rather than derived), the relevant periodic core mode of the metron model represents an integral component of the soliton system itself.

The metron model was first developed in a four-part paper using inverse modelling methods ([23] - [26], referred to in the following as H; see also [27], [28] and [34]). The solitons were treated
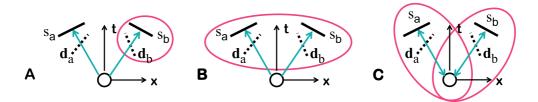
Figure 1. *Alternative interpretations of the EPR experiment. A: a hidden-variable local model (disentangled, in disagreement with experiment); B: the quantum theoretical picture of space-like entanglement; C: a time-symmetrical classical model with past-future entanglement.*

as perturbations superimposed on a constant background metric. However, explicit numerical solutions, illustrating the nonlinear wave-guide/trapped-mode interactions that lead to solitons, were presented only for a simpler scalar analogue of the Einstein equation. The number of dimensions and metric signature of extra-space were also left open.

In the present paper, we present now numerical solutions for the full system (1). The solutions confirm the basic concepts of H, but yield also a number of new insights and important modifications of the original metron model. In particular, a background wave field has been introduced that defines the basic physical constants of the theory (the vacuum eqs. (1) contain no physical constants apart from the velocity of light), as well as resolving a number of other open questions listed in H.

Our overview in Sections 3 and 4 of the application of the metron model both for the computation of elementary particles and the interpretation of quantum phenomena at lower energy levels necessarily omits many technicalities. More detailed expositions are in preparation. The last Section 5 concludes with a summary of the basic metron concepts in relation to quantum field theory.

2. Entanglement

Entanglement – the apparent conflict with causality of the measured correlation between space-like separated particles, or other objects, emitted from a common state – is widely regarded as a defining property of quantum theory [41], [38], [20]. Particles originating from a common state will necessarily be correlated; they are termed entangled if the correlation violates causality in the sense assumed by Bell in the derivation of his inequality relation. Bell's theorem was derived for classical particles under the locality condition that measurements performed on space-like separated particles are independent. In the case of the EPR experiment, the quantum theoretical prediction $C_{ab} = -\cos(\mathbf{d}_a\mathbf{d}_b)$ of the correlation between the spins s_a, s_b of two particles measured with Stern-Gerlach magnets oriented in the directions $\mathbf{d}_a, \mathbf{d}_b$, respectively, violates Bell's inequality relation. Experiments [18], [2] have clearly confirmed the quantum theoretical prediction. Thus the EPR system is entangled, and cannot be explained by a classical model satisfying the locality condition.

Although locality appears to be a self-evident requirement of causality, it corresponds, in fact, to the traditional concept of causality only for macrophysical systems characterized by an arrow of time. On microphysical scales, locality is in conflict with the more fundamental condition of time-reversal symmetry. Entanglement is found to be a universal feature of time-symmetrical microphysics, whether quantal or classical. However, the implications of time-reversal symmetry for microphysical systems are rather counterintuitive and require a more careful inspection of the concept of causality.

The alternative interpretations of the EPR experiment are illustrated in Figure 1. The left panel A corresponds to the classical hidden-variable model discussed by Bell, assuming

independence of the two spin measurements. The diagram is based on directed arrows-of-time connecting the emission and measurement processes.

The middle panel B corresponds to the standard quantum theoretical interpretation, in which the spin measurement s_a of particle a leads to a simultaneous collapse of the state vectors for both particles a and b. Entanglement appears in this representation as a causality-violating space-like phenomenon directly connecting the two measurement processes.

The right panel C represents the interpretation of entanglement for a classical model exhibiting time-reversal symmetry. A change in the orientation $\mathbf{d}_b$ of the Stern-Gerlach magnet for the second particle b affects not only the local measurement s_b, but the entire trajectory of particle b, from the time of emission to the time of detection. This modifies the emission process itself, and thereby also the emission of the first particle a and the resultant spin measurement s_a. Thus, the entire experiment, from the common emission process to the final particle measurements, is seen as a single, coupled, time-symmetrical system.

Time-reversal symmetry has been evoked by Costa de Beauregard [8], Davidson [10], Cramer [9] and Basini et al [4] to *interpret* quantum theoretical entanglement. However, it has apparently not been generally recognized that time-reversal symmetry implies entanglement for essentially all systems, whether classical or quantal. The debate on the foundations of quantum theory is thereby *circumvented*, opening the door to the development of a general classical theory unifying all forces of nature

The implications of time-reversal symmetry for classical microphysical systems are best illustrated by the photon version of the EPR experiment, in which two photons rather than particles are emitted from a common initial state. We assume that in the classical theory, the electromagnetic far fields of particles correspond (as in the case of the metron model) to the standard electromagnetic fields of classical point-like particles.

The requirement that total four momentum is conserved for a finite set of interacting point-like particles that are initially far separated, and diverge again after interacting via their far fields, implies that the interactions between the particles must be represented by time-symmetrical potential functions composed of equal advanced and retarded components. This was pointed out already by Einstein [14] in an exchange with Ritz [40], who had advocated augmenting Maxwell's equations by an outgoing radiation condition. Ritz's view is consistent with the observed radiation of accelerated charged particles to space, but violates the conservation of four-momentum for a closed system of interacting particles. Einstein's view was supported by Tetrode [44], Frenkel [19] and Fokker [17]. It was developed in detail later by Wheeler and Feynman [46], [47], who explained the observed radiative damping by interactions with a distant ensemble of absorbing particles. A generalization to gravitational interactions has been given by Hoyle and Narlikar [30]. Einstein's view, based on time-reversal symmetry, is now generally accepted.

Figure 2 illustrates the time-symmetrical electromagnetic coupling between two particles a and b travelling on trajectories $x_a^\lambda = \xi_a^\lambda(\sigma_a), x_b^\lambda = \xi_b^\lambda(\sigma_b)$. The coupling occurs along both branches of the light cone $\xi_{ab}^2 = \xi_{ab}^\lambda \xi_{ab}^\mu \eta_{\lambda\mu} = 0$, where $\xi_{ab}^\lambda = x_a^\lambda - x_b^\lambda$ and $\eta_{\lambda\mu} = \text{diag}(+1,-1,-1,-1)$ (the summation convention is applied only to tensor indices, in this case λ, μ).

The coupled equations for the rate of change of the particle momenta p_a^λ, p_b^λ (ignoring the singular field-particle self-interactions at the locations of the particles, which in a complete theory, including the finite particle core, are treated as a regular part of the internal particle structure, cf Section 3) are given by [47]

$$\frac{dp_a^\lambda(x_a)}{d\sigma_a} = \int K_{ab} \frac{\partial}{\partial \xi_{a\lambda}} [\delta(\xi_{ab}^2) p_b^\mu p_{a\mu}] d\sigma_b \tag{3}$$

with a second equation in which a and b are interchanged. $K_{ab} = K_{ba}$ denotes a symmetrical coupling expression dependent on the individual particles' mass m and charge q (in cgs-
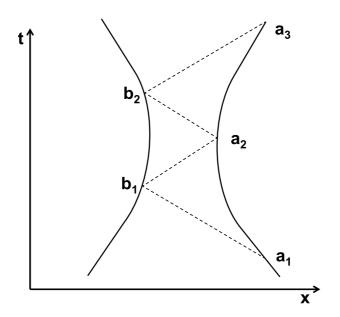
Figure 2. *Past-future entanglement in relativistic time-symmetrical systems. The acceleration of particle a at position a_2 depends on the states of particle b at both positions b_1 and b_2 on the backward and forward light cones (dashed lines), respectively. The interactions $a_1 \leftrightarrow b_1, b_1 \leftrightarrow a_2, a_2 \leftrightarrow b_2, b_2 \leftrightarrow a_3$ represent a local time-symmetrical transfer of four-momentum in accordance with the relativistic generalization of Newton's third law actio = reactio.*

ESU units, $K_{ab} = q_a q_b (m_a m_b)^{-1}$). The path variables are normalized by the condition $(d\xi^\lambda/d\sigma)(d\xi_\lambda/d\sigma) = 1$. For simplicity, the particle spin (included in the full metron model, Section 3) has been ignored.

Since

$$\frac{\partial}{\partial \xi_{a\lambda}}[\delta(\xi_{ab}^2) p_b^\mu p_{a\mu}] = -\frac{\partial}{\partial \xi_{b\lambda}}[\delta(\xi_{ab}^2) p_b^\mu p_{a\mu}], \tag{4}$$

it follows that

$$\Delta p_a^\lambda = \int \frac{dp_a^\lambda}{d\sigma_a} d\sigma_a = -\Delta p_b^\lambda = -\int \frac{dp_b^\lambda}{d\sigma_b} d\sigma_b \tag{5}$$

Thus $p_a^\lambda + p_b^\lambda$ is conserved – in accordance with the principle *actio = reactio*.

We note that the relativistic generalization of Newton's third law applies already at the local level: the conservation of momentum holds for the interactions at all particle-pair positions connected by positive or negative light cone segments (Figure 2):

$$\delta(\frac{dp_a^\lambda}{d\sigma_a}) d\sigma_a = -\delta(\frac{dp_b^\lambda}{d\sigma_b}) d\sigma_b \tag{6}$$

Thus, although it is customary to speak of a photon travelling from particle a to particle b (or from b to a), the interaction is, in fact, completely time symmetrical, the photon representing rather an entanglement between each pair of light-cone-connected particle states[1].

---

[1] Not addressed here is the basic quantum theoretical result that for a periodic electromagnetic field, the momentum transfer is quantised. Following Einstein [15], this can be attributed within the framework of a quasi-classical model (a fully classical interpretation is outlined in Section 4.2) to the discrete structure of the atomic states from which the electromagnetic radiation emanates. For the present discussion, however, the extension of the present two-particle interaction picture to include these interactions - which again underly time-reversal symmetry – is irrelevant.

The implications of time-reversal symmetry and past-future entanglement for the concept of causality have been discussed in detail by Wheeler and Feynman [47]. Although counter-intuitive, it leads to no logical contradictions, provided the application of the familiar concept of an arrow of time is systematically replaced by a time-symmetrical picture.

The application of these concepts to the photon version of the EPR experiment is straightforward. The "particles" a and b in Figure 1 represent photons coupling the intial and final electron states in the emission and detection systems, respectively, the transmitted photons being filtered by the polarization filters $\mathbf{d}_a$, $\mathbf{d}_b$. The initial and final states are thus directly "entangled", in accordance with Figure 1C.

The same picture applies also to the particle version of the EPR experiment, although in this case the time-symmetrical coupling of the initial and final states is less transparent. However, it is sufficient to recognize that also in this case the central assumption of Bell's analysis, namely the independence of the initial emission process on the later measurement process, implies an arrow of time, and is therefore inapplicable for time-symmetrical systems.

3. The metron model

3.1. The Einstein vacuum equations

Having established that Bell's theorem is no hindrance to the development of a classical theory of quantum phenomena, we turn now to the metron model. We seek a representation of elementary particles as soliton solutions of the twelve-dimensional Einstein vacuum equations (1), without a cosmological term. The equations may be written alternatively in the Ricci-flat form

$$R_{LM} = 0, \tag{7}$$

where

$$R_{LM} = \partial_M \Gamma^N_{LN} - \partial_N \Gamma^N_{LM} + U_{LM} \tag{8}$$

is the Ricci curvature tensor, with

$$U_{LM} = \Gamma^N_{LO}\,\Gamma^O_{MN} - \Gamma^N_{LM}\,\Gamma^O_{NO}, \tag{9}$$

$$\begin{aligned}
\Gamma^L_{MN} &= \frac{1}{2}\,g^{LO}\,[\partial_M g_{ON} + \partial_N g_{OM} - \partial_O g_{MN}] \\
&= g^{LO}\Gamma_{OMN},
\end{aligned} \tag{10}$$

and where

$$\Gamma_{OMN} = \frac{1}{2}\,[\partial_M g_{ON} + \partial_N g_{OM} - \partial_O g_{MN}] \tag{11}$$

is the affine connection of the metric tensor.

Essential for our approach is the exclusion of the matter-dependent source terms. This enables particles to be *derived* as the soliton solutions of eq.(1), rather than being *specified a priori* through the source terms.[2]

We make a second important assumption, following Klein [33]: all fields are assumed to be periodic (or constant) with respect to extra-space and time (in the soliton restframe). The extra-space and temporal periodicities are prescribed; they will be identified with the particle masses and generalized charges. The periodicity assumption reduces the problem of solving the twelve-dimensional Einstein equations to a three-dimensional problem. In the particle models

---

[2] This is also in the spirit of Einstein, who is said to have the regarded the matter-dependent energy-momentum source term tensor of his equation as "plywood" compared to the "marble" of the geometrical curvature term.

presented below, the dimensionality is reduced further to one by assuming spherical symmetry with respect to physical space.

Formally, the periodicity assumption with respect to extra-space implies that the twelve-dimensional manifold can be represented as a bundle [43],[21],[31] composed of an eight-dimensional fibre (extra-space), dependent on a small number of discrete wavenumber parameters, defined over a four-dimensional base space (spacetime). The periodicity ansatz avoids also the need to compactify extra-space onto a very small Planck sphere in order to explain why we experience physics in only four dimensions. In this respect our approach differs from string theory and other higher-dimensional models.

We derive the metric soliton solutions as perturbations

$$g'_{LM} = g_{LM} - \eta^{(b)}_{LM} \tag{12}$$

of the metric g_{LM} relative to a homogeneous background metric $\eta^{(b)}_{LM}$. The latter is assumed to consist of a superposition

$$\eta^{(b)}_{LM} = \eta_{LM} + \tilde{\eta}_{LM} \tag{13}$$

of a constant diagonal metric

$$\eta_{LM} = \mathrm{diag}(+1, -1, -1, -1, -1, ..., -1, +1) \tag{14}$$

and a background free-wave field $\tilde{\eta}_{LM}$.

The first four components $\eta_{00}, \ldots, \eta_{33}$ of the mean background metric (14) refer to physical spacetime. We use natural units: $c = 1$, and (in wavenumber-dependent expressions below) $\hbar = 1$. The spacetime signature pattern is repeated in the metric components $\eta_{44}, \ldots, \eta_{11,11}$ of the fibre, the first seven of which have negative sign, while the sign of the last component is again positive.[3]

The spacetime components of the metric perturbation g'_{LM} represent the normal gravitational field, while metric-tensor components with fibre-only or mixed spacetime-fibre indices will be identified with fermion and boson fields, respectively.

The introduction of a background free-wave field $\tilde{\eta}_{LM}$ represents an important extension of the original metron model (H). The wave field consists of a continuum[4]

$$\tilde{\eta}_{LM} = \sum_w \eta^{(w)}_{LM} = \sum_w B^{(w)}_{LM} \exp i(k^{(w)}_N x^N) \tag{15}$$

of statistically independent wave components $\eta^{(w)}_{LM}$ of amplitude $B^{(w)}_{LM}$ whose wavenumbers satisfy the dispersion relation

$$k^{(w)}_L k^{(w)}_M \eta^{LM} = 0. \tag{16}$$

of linear waves on the twelve-dimensional bundel. The fibre wavenumber components k_L, $L = 4, \ldots, 11$ consist of a prescribed discrete set identical to the fibre wavenumber components of the soliton solutions. They represent the generalized particle charges. The spacetime wavenumbers k_L, $L = 0, \ldots, 3$ consist of a continuum lying on three-dimensional subspaces corresponding to the particle masses.

---

[3] In the inverse analysis of H, both a Euclidean and a Minkowski-type extra-space metric were considered. However, it was found that the Euclidean metric fails to yield soliton solutions of the full tensor equations (1). The possible occurrence of tachyons in non-Euclidean higher-dimensional gravity theories is irrelevant for the metron model, as the periodic higher dimensional space serves only as a template for deriving field equations in four-dimensional spacetime.

[4] Following common practice, we write the statistical continuum of wave components as a sum rather than as a formally more correct (but more cumbersome) Fourier-Stieltjes integral.

The inclusion of a background wave field resolves a number of open questions, listed partially already in H: 1) by assuming that the background wave field exhibits the same periodicities as the metron solutions, it enables the introduction of the basic physical constants lacking in the vacuum equations (1) themselves; 2) it ensures the uniqueness and stability of the metron solutions; 3) it removes, through selective attenuation, a spurious super strong far-field component that had concerned already Kaluza [32] in his five-dimensional generalization of Einstein's equation, and 4) it explains the left-handed polarity of the weak interactions and the finite masses of the weak-interaction gauge bosons in terms of interactions with a sub-set of background field components exhibiting these properties.

We consider the role of interactions with the background wave field later in Section 3.5, after we have presented the basic properties of the metron soliton solution for a constant background metric.

To obtain unique solutions, the Einstein equations, with appropriate boundary conditions, must be augmented by additional gauge conditions [37]. We choose the usual Lorentz gauge, the divergence condition

$$\partial_M h_L^M = 0, \tag{17}$$

where

$$h_{LM} = g'_{LM} - \frac{1}{2}\eta_{LM}(\eta^{NO}g'_{NO}). \tag{18}$$

represents the trace-modified metric perturbation.

Expressed in terms of h_{LM}, and applying (17), the Einstein vacuum equations (1) then take the general form

$$\Box_n h_{LM} = q_{LM}, \tag{19}$$

where $\Box_n = \partial_N\partial_O\eta^{NO}$ denotes the higher-dimensional box operator and q_{LM} are nonlinear source terms.

Formally, q_{LM} represent the gauge-field interactions that ensure the invariance of the Einstein equations with respect to coordinate transformations. However, this property, although important in comparing the formal structure of the higher-dimensional Einstein-Hilbert Lagrangian underlying the metron model with the Standard Model Lagrangian of quantum field theory (cf. H), is irrelevant for the present discussion. For our purposes, it is sufficient to note that the perturbation expansions of the source terms q_{LM} begin with quadratic terms and are homogeneous of second order with respect to the derivatives. The algebra of the perturbation expansion can then be summarized in terms of interaction diagrams, with associated simple rules for the computation of the various vertex contributions (cf. Section 3.3).

The traces of the fields g'_{LM} and h_{LM} are found to be very small, so that $g'_{LM} \approx h_{LM}$. Results will be presented for h_{LM}, but can equally be interpreted as representing g'_{LM}.

3.2. The soliton dynamics

The system (19) supports soliton solutions consisting of periodic nonlinear eigenmodes that are trapped in a wave guide. The soliton structure differs significantly from the familiar Korteweg-de Vries balance between linear dispersion and nonlinear amplification. The trapping wave guide h^g represents a distortion of the metric in which the eigenmodes h^c propagate (Figure 3). It is generated by the radiation stresses of the trapped eigenmodes. The eigenmodes (*core* modes) are concentrated in the strongly nonlinear metron core, decreasing exponentially for larger distances r from the core, while the non-periodic wave-guide far fields fall off as $1/r$.

For periodic, spherically symmetric soliton solutions, the system (19) reduces to a set of coupled equations of the general form
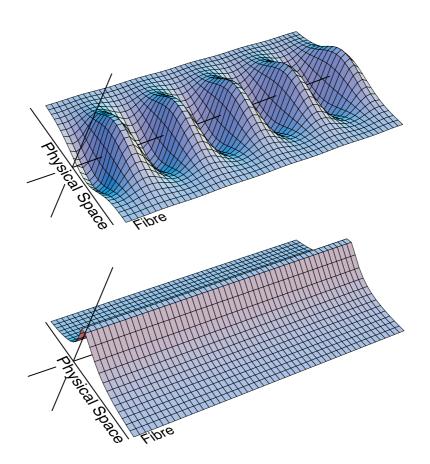
Figure 3. *Schematic diagram of the periodic trapped-mode (upper panel) and wave-guide (lower panel) components of a metric soliton in the product space physical-space × fibre (from H). The trapped core modes are periodic also with respect to time.*

$$\left(\frac{d^2}{dr^2} + \frac{2}{r}\frac{d}{dr} - (\kappa^{(c)})^2 + u^{(c)}(h^{(g)}) \right) h^{(c)}(r) = 0 \qquad \text{(core modes)} \qquad (20)$$

$$\left(\frac{d^2}{dr^2} + \frac{2}{r}\frac{d}{dr} \right) h^{(g)}(r) = q^{(g)}(h^{(c)}) \text{ (wave guides)} \qquad (21)$$

where $h^{(c)}$ denote the amplitudes of the fundamental periodic core modes of the soliton, $h^{(g)}$ are non-periodic wave-guide fields generated by quadratic difference interactions, $u^{(c)}(h^{(g)}), q^{(g)}(h^{(c)})$ represent nonlinear interaction terms, and

$$(\kappa^{(c)})^2 = -k_L^{(c)} k^{(p)L} = -(k_0^{(c)})^2 + \sum_{L=4}^{10} (k_L^{(c)})^2 - (k_{11}^{(c)})^2. \qquad (22)$$

The parameter $\kappa^{(c)}$ determines the asymptotic exponential fall-off rate of the core mode and thus the effective spatial scale of the soliton solution.

We have suppressed the tensor structure of the fields, which slightly modifies the spherically symmetric form of the Laplace operator for the wave-guide components, and have similarly ignored small modifications of the spherically symmetric equations for solitons composed of several spinor core-mode components (cf. Section 3.7.1). Not included in eq (20) are also interactions with the second-harmonic fields and the direct cubic interaction term, both of which are formally of the same perturbation order as the interaction with the wave-guide field. These
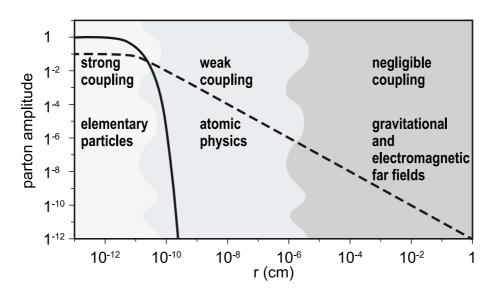
Figure 4. *Near- and far-field components of metron solutions. Full line: core modes (fermions), decreasing exponentially for large r; dashed line: wave-guide fields (massless bosons), decreasing asymptotically as 1/r.*

interactions are neglible under the second of the following two inequality conditions, which are found to be essential for the existence of soliton solutions:

$$0 < (\kappa^{(c)})^2 \ll (k_L^{(c)})^2, \ L = 0, 4, 5, \ldots 11, \tag{23}$$

The left inequality is necessary in order that the core modes are localized in the soliton core, falling off exponentially for large r. The right inequality implies that $|dh^{(c)}/dr| \ll |k_L^{(c)} h^{(c)}|$, $L = 0, 4, 5, \ldots 11$. This turns out to be a key condition both for the convergence of the iterative construction of numerical solutions of the system (20), (21) and for the identification of the wave-guide far fields with the classical electromagnetic and gravitational far fields of point-like particles.

The basic core-mode/wave-guide interaction mechanism is independent of the details of the tensor and periodicity structure of the soliton solutions. However, these properties are important for the mapping of the different soliton components into the associated classes of elementary particles. We distinguish in the following between tensor indices $L, M, \ldots$ of the full twelve-dimensional bundle, fibre tensor indices $l, m, \ldots$, spacetime indices $\lambda, \mu, \ldots$ and physical-space indices $\bar{i}, \bar{j}, \ldots$.

Core-mode components are identified with fermions, wave-guide components with bosons (Figure 4). The mapping relations of the tensor components are listed in Table 1, while the associated wavenumber components are shown in Figure 5. Fermion fields h_{lm} lie in the fibre domain $8 \leq l, m \leq 10$; the associated wavenumbers k_L lie in the complementary index domain $L < 8$ and $L = 11$. This ensures that the fermion core-mode fields satisfy the gauge condition (17). Boson fields h_{0l} lie in the mixed-index domain $4 \leq l \leq 7$; the field $h_{0,0}$ corresponds to the standard gravitational field (in the particle restframe) of general relativity. Anti-particles are represented by an inversion of the fibre, i.e. by a change in sign of the fibre wavenumber components.

The four quantum-theoretical spinor components, represented by left and right handed Weyl two-spinors φ_1^L, φ_2^L and φ_1^R, φ_2^R, respectively, are mapped into metric tensor components in the fermion sector in accordance with the scheme (representing one particular realization of the
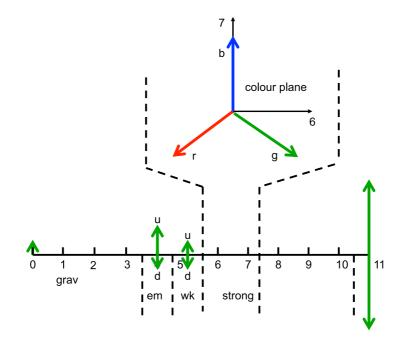
Figure 5. *Wavenumber components* $(k_0, k_4 - k_7, k_{11})$ *of fermions (leptons and up and down quarks). Each fermion is composed of mirrored core-mode pairs with equal wavenumber components* k_L *for* $L < 11$ *and opposite wavenumber components* $\pm k_{11}$.

Indices	0-3	4	5	6,7	8,9,10	11
0 - 3	grav	el-magn	weak	strong	-	-
4	el-magn	KSS	KSS	KSS	-	KSS
5	weak	KSS	KSS	KSS	-	KSS
6,7	strong	KSS	KSS	KSS	-	KSS
8,9,10	-	-	-	-	fermion	-
11	-	KSS	KSS	KSS	-	KSS

Table 1. Mapping of metron components into gravitational fields, fermions, electromagnetic, weak and chromodynamic (strong) bosons, and KSS fields.

mapping of the five independent components of a traceless metric h_{lm}, $l, m = 8, 9, 10$ into four spinor components):

$$\begin{pmatrix} h_{88} & h_{89} & h_{8,10} \\ h_{98} & h_{99} & h_{9,10} \\ h_{10,8} & h_{10,9} & h_{10,10} \end{pmatrix} = \begin{pmatrix} 0 & \varphi_1^L & \varphi_2^L \\ \varphi_1^L & \varphi_2^R & \varphi_1^R \\ \varphi_2^L & \varphi_1^R & -\varphi_2^R \end{pmatrix} \tag{24}$$

The metron picture yields a simple explanation of the Fermi-Dirac and Bose-Einstein statistics of fermions and bosons, respectively. Since fermions represent strongly nonlinear fields localised in the particle core, they cannot be superimposed with the core fields of other particles within the same particle core. Bosons, in contrast, represent far fields, which can be readily superimposed beyond the particle core regions.

In addition to the standard gravitational and quantum theoretical fields, Table 1 includes the afore-mentioned spurious Kaluza Super Strong (KSS) fields in the non-mixed fibre-index sector
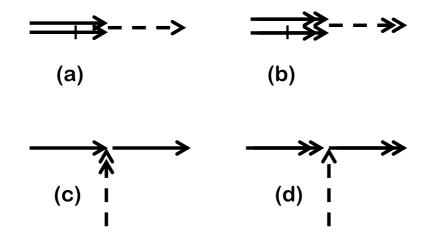
Figure 6. *Panels (a), (b): generation of wave-guide fields (dashed arrows) by quadratic interactions of core modes (full arrows) and mirrored core modes (double-headed arrows). Cross-bars denote complex-conjugate fields (not anti-particles). Panels (c), (d): feedback of wave-guide fields on the eigenvalues of core modes. The dominant feedbacks are cross-interactions between core modes and wave-guide fields generated by mirrored core modes.*

complementary to the fermion sector. It will be shown in Section 3.5 that these are effectively removed through interactions with the background wave field.

The wavenumbers k_L represent generalized particle charges. The wavenumbers k_0, k_4, correspond to the particle mass and electric charge, respectively, the associated wave-guide far fields h_{00}, h_{04} representing the classical gravitational and electromagnetic far fields of a point-like particle (cf. Section 3.4). The weak iso-charge and strong coupling coefficients are given, respectively, by the wavenumbers k_5 and wavenumber vectors $\mathbf{k}_r, \mathbf{k}_b, \mathbf{k}_g$ in the colour plane $k_6.k_7$, where $\mathbf{k}_r + \mathbf{k}_b + \mathbf{k}_g = 0$ (cf. Figure 5). In analogy with Einstein's four-dimensional general relativity, k_0 plays a dual role of representing both the gravitational and inert mass.

It is shown in the next section that the wave-guide far fields h_{0L}, $L = 0, 4, 5, \ldots, 10$ are proportional to the wavenumber products $k_0 k_L$, with a common proportionality factor. The empirical result that the electromagnetic forces greatly exceed the gravitational forces implies then $k_4 \gg k_0$ (for the electron, for example, $k_4/k_0 \approx 1.4\ 10^{21}$). The right-hand inequality (23) can be satisfied in this case only if the core-mode wavenumber vector includes a component, k_{11}, say, of approximately the same magnitude as k_4, but of opposite metric signature. This is the motivation for the introduction of a positive time-like sign for the last metric component $\eta_{11,11}$. Since a net force corresponding to $h_{0,11}$ is not observed, however, the soliton must contain two "mirrored" core-mode constituents of the same amplitude, whose last wavenumber components k_{11} have opposite signs, but whose wavenumbers are otherwise identical[5]. This results in a cancellation of the net boson far field $h_{0,11}$, while the gravitational, electromagnetic and other far fields are not affected.

3.3. Interaction diagrams
The interactions between core-mode and wave-guide fields can be conveniently summarized in terms of interaction diagrams (Figure 6). Core-mode fields are represented by full arrows, wave-guide fields by dashed arrows. A double-headed arrow represents the mirrored core

---

[5] Instead of introducing two mirrored components $h_{L,11} \sim \exp(\pm i k_{11} x^{11})$, one could, of course, equivalently consider a single component $h_{L,11} \sim \cos(k_{11} x^{11})$. For interaction computations, however, it is more convenient to work with two complex exponentials.

mode of a core-mode pair, or the wave-guide field generated by a mirrored core mode. Cross-bars denote complex-conjugate fields of the same particle (as opposed to the usual Feynman-diagram notation for anti-particles). Arrow directions indicate the sequence in the perturbation expansion; the interactions themselves are time-symmetrical.

The coupling coefficients associated with a vertex consist of contractions of tensor expressions composed of quadratic products of the wavenumber components of any of the incident fields multiplied by the incident field amplitudes. This yields a forcing of the gravitational, bosonic and KSS wave-guide fields $h_{00}^{(g)}$, $h_{0l}^{(g)}$ and $h_{lm}^{(g)}$ proportional to the square of the core-mode amplitude times k_0^2, $k_0 k_l$ and $k_l k_m$, respectively, with a common proportionality factor.

The very large ratios k_l/k_0, mentioned above as motivation for the introduction of a time-like fibre metric signature to satisfy the inequality (23), presents now a further problem: it implies very large KSS fields in the pure fibre sector compared with the bosonic fields of the mixed spacetime-fibre sector (cf. Table 1). The KSS fields are not observed; they will be removed in Section 3.5 through interactions with a background wave field. Before addressing this problem, however, we investigate first the implications of the wave-guide far fields for the interactions between well separated particles.

3.4. Far-field interactions

So far, we have considered only an isolated particle at rest at the location $\mathbf{x} = 0$. We consider now the forces produced by the interaction of the particle with the wave-guide far fields g_{LM}^F of another distant particle (or of several such particles).

According to higher-dimensional general relativity, the force experienced by a particle propagating with the velocity v^L in a perturbed higher-dimensional metric

$$g^{LM} = \eta^{LM} - g_{NO}^F(x)\eta^{LN}\eta^{MO} + \cdots \tag{25}$$

can be represented by the geodetic acceleration

$$\frac{dv^L}{ds} = -\Gamma_{MN}^L v^M v^N. \tag{26}$$

Applied to the spacetime velocity components (the rate of change of the fibre velocity components is irrelevant due to the assumed homogeneity on the fibre), this yields

$$\frac{dv^\lambda}{ds} = -\Gamma_{\mu\nu}^\lambda v^\mu v^\nu + F_{\mu l}^\lambda v^\mu v^l + K^\lambda, \tag{27}$$

where the first term on the right hand side represents the standard Einstein gravitational acceleration in physical spacetime, the second term the acceleration due to the mixed-index (i.e. bosonic, cf. Table 1) far fields

$$F_{\mu l}^\lambda = \eta^{\nu\lambda}\left(\partial_\nu g_{\mu l} - \partial_\mu g_{\nu l}\right), \tag{28}$$

or

$$F_{\mu l}^\lambda = \partial^\lambda A_{\mu l} - \partial_\mu A_l^\lambda \quad \text{with} \tag{29}$$
$$A_{\lambda l} = g_{\lambda l}, \tag{30}$$

and the third term represents the Kaluza super strong (KSS) acceleration

$$K^\lambda = \frac{1}{2}\eta^{\nu\lambda}\partial_\nu g_{lm} v^l v^m \tag{31}$$

produced by the far fields g_{lm}^F in the fibre sector.

The bosonic acceleration expressions (28) - (30) have a structure analagous to the Lorentz force

$$m \, dv^\lambda/ds = e\hat{F}_\mu^\lambda v^\mu (v_\nu v^\nu)^{1/2} \tag{32}$$

where m and e denote the particle's mass and charge, respectively, and

$$\hat{F}_\mu^\lambda = \partial^\lambda \hat{A}_\mu - \partial_\mu \hat{A}^\lambda \tag{33}$$

is the electromagnetic field, expressed in terms of the electromagnetic potential $\hat{A}_\lambda$.

Before proceeding, we must first define what is meant by the velocity v^L in twelve-dimensional space of a "particle" that corresponds to the classical concept of a localized point-like particle in physical spacetime, but represents a homogeneous periodic wave field with respect to the fibre. A consistent definition can be obtained by formally relaxing the homogeneity of the periodic field with respect to the fibre and considering instead a finite-extent wave group of scale R that satisfies the WKB conditions $|k_l|R \ll 1$. The metron particle can then be treated as a 12-dimensional wave group propagating with the group velocity

$$v^L = \partial\Omega/\partial k_L, \tag{34}$$

where $\Omega(x,k) = 0$ represents the dispersion relation of waves in the perturbed twelve-dimensional space:

$$\Omega(x,k) = g^{LM}(x)k_L k_M = 0, \tag{35}$$

with $g^{LM}(x)$ given by eq. (25).

The group velocity is accordingly

$$v^L = 2\eta^{LM}k_M \tag{36}$$

The metron relations (28) - (30) can then be recognized as the generalization of the Lorentz electromagnetic force to all bosonic forces, where the wavenumbers represent, as mentioned above, the generalized charges of the various fields. In particular, the metron expressions for the gravitational and electromagnetic accelerations map into the corresponding classical expressions by applying scaling factors ρ_1, ρ_2, ρ_3:

$$
\begin{align}
A_{\lambda 4} &= \rho_1 \hat{A}_\lambda \tag{37}\\
F_{\mu 4}^\lambda &= \rho_1 \hat{F}_\mu^\lambda \tag{38}\\
k_4 &= \rho_2 \, e \tag{39}\\
k_0 &= \rho_3 \, m, \tag{40}
\end{align}
$$

where the scaling factors satisfy the condition

$$\rho_3 = \rho_1 \rho_2. \tag{41}$$

The scaling factors depend on the choice of units in the metron and standard classical theories. We identify the rest-frame frequency k_0 with the mass m via the Planck relation $k_0 = mc/\hbar$, or, in natural units, $k_0 = m$. Thus,

$$\rho_3 = c/\hbar = 1 \quad \text{in natural units.} \tag{42}$$

so that eq. (41) reduces to

$$\rho_1 \rho_2 = c/\hbar = 1 \quad \text{in natural units.} \tag{43}$$

Similar scaling factors apply for the relevant relations for the weak interactions (coupling constant k_5) and strong forces (coupling wavenumbers $\mathbf{k}_r, \mathbf{k}_b, \mathbf{k}_g$) that will be considered after we have presented numerical metron solutions in Section 3.6 (the remaining wavenumber k_{11} yields no net force, as pointed out above, since the mixed-index fields $g_{\mu,11}$ occur in cancelling mirrored pairs). It is found that the free parameters of the metron model (basically, the scale $\kappa^{(c)}$ of eq. (22) and the energy level of the background wave field) can be chosen such that the scaling parameters $\rho_1, \rho_2, \ldots$ for all bosonic forces are in agreement with experiment.

There remains the KSS force. A comparison of eqs.(31) and (29) reveals, as pointed out already by Kaluza, that, considering alone the contributions to K^λ from the metric components g_{44}, the KSS force exceeds the electromagnetic force by a factor of the order $g_{44}k_4/g_{04}k_0$. Since the ratio g_{44}/g_{04} for the fields alone is already of order k_4/k_0, as pointed out in the previous section, we obtain for the force ratio $K^\lambda/(F_\mu^{\lambda(em)} v^\mu) = O\{(k_4/k_0)^2\} \approx 2\,10^{42}$ for the electron. For a viable theory, the KSS fields must therefore clearly be removed by some mechanism. This is achieved through interactions with the background wave field.

3.5. The background wave field

A background wave field is required not only to attenuate the KSS fields, but also for the other important reasons mentioned earlier. We summarize in the following only the basic concepts.

Statistical homogeneity implies for the amplitudes of the wave-field representation (15)

$$< B_{LM}^{(w)} >= 0 \tag{44}$$

and

$$< B_{LM}^{(w)} B_{L'M'}^{(w')*} >= P_{LML'M'}(k^{(w)})\, \delta_{ww'}, \tag{45}$$

where the cornered parentheses denote statistical ensemble averages and $P_{LML'M'}$ represents the wave spectrum.

In contrast to the fibre wavenumbers k_l, $l = 4, 5, \ldots, 11$, which consist of a discrete set corresponding to the generalized particle charges, the spacetime wavenumber components $k_\lambda^{(w)}$, $\lambda = 0, \ldots, 3$ represent a three-dimensional continuum (since we can no longer remain in the restframe of a particular particle) satisfying the de Broglie dispersion relation

$$k_\lambda^{(w)} k_\mu^{(w)} \eta^{\lambda\mu} - m_w^2 = 0, \tag{46}$$

where the constants m_w represent (to within a small deviation of order $(\kappa^{(c)}/k_0^{(c)})^2$, cf. eq. (23), that is irrelevant here) the discrete masses of the particles. Applying eqs.(16) and (46), the fibre wavenumbers are seen to be inter-related via the particle masses:

$$k_l^{(w)} k_m^{(w)} \eta^{lm} + m_w^2 = 0. \tag{47}$$

We shall be concerned primarily with interactions between the background wave continuum and the metron soliton in the metron restframe, in which the metron spacetime wavenumber vector reduces to the metron frequency k_0 (i.e. the metron mass), with $\mathbf{k} = (k_1, k_2, k_3) = 0$. Important for the question of the particle stability is then the background wave spectral density $P_{LML'M'}(\mathbf{k}^{(w)})$ at $\mathbf{k}^{(w)} \approx 0$, where the frequencies $k_0^{(w)}$ of the background wave field and metron core mode are sufficiently close that the two fields can exchange energy through resonant interactions. However, other background wave components with $\mathbf{k} \neq 0$ can engage in a resonant energy transfer at higher interaction order. The full background spectrum enters also in the computation of the damping factors for the KSS far fields, which is not dependent on resonant interactions.
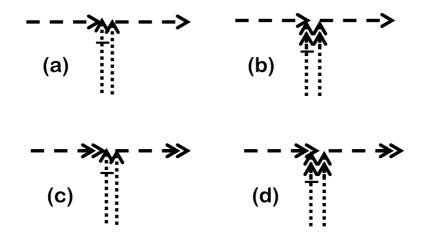
Figure 7. *Selective damping of KSS fields (dashed arrows) through interactions with background wave fields (dotted arrows). Panels (a), (b): damping of KSS fields by cubic interactions with the background wave fields and their mirrored partners. Panels (c),(d): analagous diagrams for the damping of the mirrored KSS fields.*

Important for the interactions with the background wave field are not only their wavenumbers, but also their polarization properties. We assume that these correspond to fermion fields, i.e. that the tensor indices of the background waves $B_{LM}^{(w)}$ lie in the domain $8 \le L, M \le 10$.

The general structure of the various interactions with the background wave field are summarized in the following in terms of interaction diagrams.

3.5.1. The KSS damping mechanism
Figure 7 depicts the interactions that lead to a selective attenuation of the KSS fields. All wave-guide fields, which are themselves generated by quadratic difference interactions of the basic core-modes (Figure 6), experience an additional quadratic difference interaction with the background wave field. This yields a modified field equation for the KSS wave-guide fields of the form

$$\left(\frac{d^2}{dr^2} + \frac{2}{r}\frac{d}{dr} \right) h_{lm} - Dk_l k_m h_n^n = q_{lm}, \tag{48}$$

where D is a positive damping coefficient given by an integral over the background wave spectrum (45).

Essential for the selective damping of the KSS fields is the proportionality of the damping term to the fibre wavenumber product $k_l l_m$. This implies that the damping of the KSS fields, which is proportional to quadratic fibre wavenumber products, is very much larger than the analagous damping expressions for the boson fields, which contain at most one fibre wavenumber component. Thus, for the KSS field h_{44}, for example, the damping is a factor k_4/k_0 larger than the damping of the electromagnetic far field h_{04}, and of order k_4^2/k_0^2 larger than the damping of the gravitational field (cf. eq. 27). For a suitable choice of the the damping factor (i.e. of the energy density of the background wave spectrum) the KSS fields can thus be effectively attenuated within a scale of the order of the soliton-core scale $(\kappa^{(c)})^{-1}$, while the electromagnetic and gravitational far fields remain unaffected.

3.5.2. Uniqueness and stability of the metron solutions
The coupled core-mode/wave-guide system (20), (21) yields a continuum of possible soliton solutions, given an arbitrary set of fibre wavenumbers, provided only that the wavenumbers
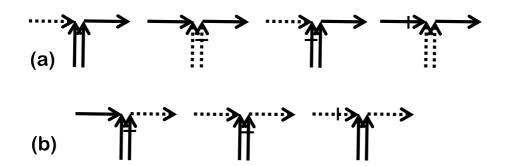
Figure 8. *Interactions ensuring stability and uniqueness of the soliton solutions.*

satisfy the inequality relations (23). In the absence of a background wave-field, however, the solutions are unstable and decay into free waves. But if there exists a background wave field, the sub-set of soliton solutions whose fibre wavenumbers are the same as those of the background wave field are stabilized through resonant interactions with the background field. The radiative losses are balanced in this case by the radiation pressure of the background waves.

The relevant interactions are summarized in Figure 8. Diagrams a show the interactions producing a net transfer of energy from the background wave field to the core mode, while diagrams b show the balancing interactions yielding a net transfer from the core mode to the background wave field (the number of interactions differ in the two cases, as it is assumed that the background wave field enters only to second order, while the core-mode interactions are retained to third order). To limit the number of diagrams, we have not differentiated in this case between mirrored partners. Starting from an arbitrary initial soliton solution with fibre wavenumber components corresponding to the background wave field, the soliton solution adjusts to a unique solution determined by the energy density of the background wave field.

A further important process is the interaction with an exceptional background wave field characterized by left-handed polarization and a relatively large frequency (mass) $m = (k_\lambda k^\lambda)^{1/2}$. This is the origin of the chirality of the weak interactions and the mass of the weak interaction gauge bosons. We return to the weak interactions in Section 3.7.4, after we have reviewed some further properties of the metron model.

3.6. A numerical metron solution
Numerical solutions of the system (20), (21) can be constructed iteratively. Starting from a first-guess core mode, one computes the wave-guide field that it generates. This enables the computation of a second-guess core mode, including the feedback from the wave-guide field, and so on. For a given background wave field and prescribed wavenumbers satisfying the inequalities (23), the solution typically converges within twenty to forty iterations.

Figures 9, 10 show the computed core-mode and wave-guide fields, respectively, for a scalar model containing only a single core mode, with wavenumbers $k_0 = 0.1, k_4 = 1000$ (corresponding to a gravitational and electromagnetic far field) and $k_{11} = \pm k_4(1 - 0.505\,10^{-8})$, yielding $\kappa = 0.01$. The model may be regarded as a rudimentary representation of the electron. It will be generalized in the next section to include the particle spin and weak interactions. The ratio $k_4/k_0 = 10^4$ (imposed by computer limitations) is considerably smaller than the real ratio $\approx 1.4\,10^{21}$ for the electron, but the computations can be readily scaled to realistic values using the scaling relations
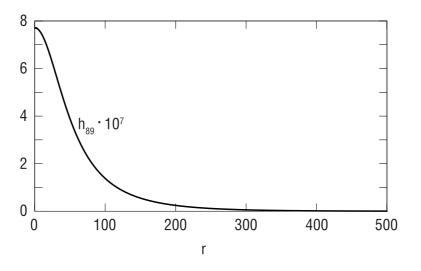
Figure 9. *Core-mode field of the scalar metron solution.*

$$h_{89}^{(c)} = \left(\frac{\kappa^2}{k_0\,k_4}\right) f_c(r) \quad \text{for the core-mode field} \tag{49}$$

$$h_{0l}^{(g)} = \left(\frac{\kappa^2 k_l}{k_0 k_4^2}\right) f_g(r) \quad \text{for gravitational and electromagnetic far fields} \tag{50}$$

$$h_{lm}^{(g)} = \frac{\kappa^2 k_l k_m}{k_0 k_4^3}\hat{f}_g(r) \quad \text{for KSS far fields.} \tag{51}$$

where

$$f_c(r) = \left\{ \begin{array}{ll} \alpha_c & \text{for} \quad r = 0 \\ \beta_c e^{-\kappa r}\,(\kappa\,r)^{-1} & \text{for} \quad \kappa\,r \gg 1 \end{array} \right\} \tag{52}$$

$$f_g(r) = \left\{ \begin{array}{ll} \alpha_g & \text{for} \quad r = 0 \\ \beta_g\,(\kappa\,r)^{-1} & \text{for} \quad \kappa\,r \gg 1 \end{array} \right\} \tag{53}$$

$$\hat{f}_g(r) = \left\{ \begin{array}{ll} \hat{\alpha}_g & \text{for} \quad r = 0 \\ \hat{\beta}_g\,e^{-\hat{\kappa} r}\,(\hat{\kappa}\,r)^{-1} & \text{for} \quad \hat{\kappa}\,r \gg 1 \end{array} \right\}, \tag{54}$$

$\alpha_c, \beta_c, \alpha_g, \beta_g, \hat{\alpha}_g, \hat{\beta}_g$ are constants of order unity, and the exponential fall-off rate $\hat{\kappa}$ of the KSS fields h_{lm}^g is given by $\hat{\kappa} = (Dk_l k_m)^{1/2}$, cf. eq.(48).

Although the exponential fall-off rate of the KSS fields yields neglible fields beyond the particle core, the KSS fields nevertheless still exceed the gravitational and electromagnetic fields within the core region itself. This is a necessary condition for the trapping of the core mode, since the electromagnetic wave-guide component, the largest non-KSS wave-guide field, has the wrong sign for trapping.

The energy level of the background wave field and the particle scale κ^{-1} (the two free parameters of the model) can be chosen such that the scalar metron solution reproduces the charge and mass of the electron, while satisfying the trapping condition and the condition that the electron scale κ^{-1} is large compared with the Compton radius $\hbar/(mc) = 3.86\ 10^{-11}$ cm (eq. 23)). The parameters can furthermore be chosen such that κ^{-1} is of the same order as the Bohr radius $\hbar^2/(e^2\,m) = 5.3\ 10^{-9}$ cm, which will be found below (Section 4.2) to be a necessary condition for the metron interpretation of atomic spectra.
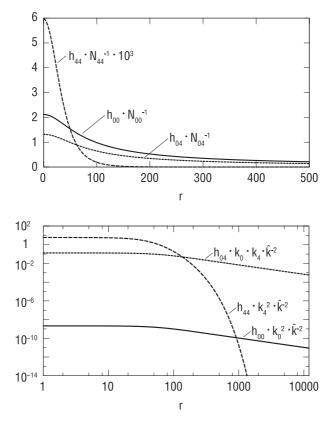
Figure 10. *Wave-guide fields of the scalar metron solution. Top panel: linear fields; bottom panel: log-log plot ($\hat{k} \equiv \kappa$; N_{44}, N_{00} are normalization factors).*

To obtain a realistic base model for the representation of the elementary particle spectrum, our model needs to be extended through the inclusion of the particle spin and the fibre wavenumber components k_5 and $\mathbf{k} = (k_6, k_7)$ representing the weak and strong interaction coupling constants, respectively. We introduce these extensions in the following section describing the metron representations of the electron, neutrino and proton/neutron system.

3.7. The first family of elementary particles
3.7.1. The electron
Spin can be introduced into the metron model by replacing the scalar core-mode component by a four-spinor field composed of left and right two-spinor fields $\psi^L = (\varphi_1^L, \varphi_2^L)$, $\psi^R = (\varphi_1^R, \varphi_2^R)$ representing metric components as defined in Table 1.

In the linear approximation, the two-spinors are coupled via the Weyl form

$$(\sigma^{\bar{i}} \partial_{\bar{i}} - \partial_t)\psi^L = i\hat{\omega}\psi^R \tag{55}$$

$$(\sigma^{\bar{i}} \partial_{\bar{i}} + \partial_t)\psi^R = -i\hat{\omega}\psi^L. \tag{56}$$

of the Dirac equation, where $\sigma^{\bar{i}}$ ($\bar{i} = 1, 2, 3$) denote the Pauli matrices and

$$\hat{\omega}^2 = -k_l^{(c)} k_{(c)}^l = (\kappa^{(c)})^2 + (k_0^{(c)})^2, \tag{57}$$

We seek as before a spherically symmetric solution. In view of the coupling relations (55), (56), we can no longer simply assume $\psi^{L,R} = \psi^{L,R}(r)$. Instead, the isotropy of a four-spinor field that

is periodic in time t, $\psi^{L,R} \sim \exp(i\omega t)$ is represented by the general form

$$\psi^L = \{-(\hat{\omega} + \omega) + i\sigma^{\bar{i}}\partial_{\bar{i}}\}f(r)\,e^{i\omega t}A \tag{58}$$

$$\psi^R = \{(\hat{\omega} + \omega) + i\sigma^{\bar{i}}\partial_{\bar{i}}\}f(r)\,e^{i\omega t}A \tag{59}$$

where $A = (A_1, A_2)$ is an arbitrary constant 2-spinor factor and the function $f(r)$ satisfies the scalar spherically-symmetric Klein-Gordon equation

$$\left\{\frac{d^2}{dr^2} + \frac{2}{r}\frac{d}{dr} + \omega^2 - \hat{\omega}^2\right\}f(r) = 0 \tag{60}$$

The relations (58)-(60) represent the linearized four-spinor generalization of the scalar eigenvalue equation (20).

The nonlinear eigenvalue equations, including the coupling to the wave-guide fields, are obtained as in the scalar case by substituting the linear form (58)-(59) into the nonlinear Einstein equations and expanding in a perturbation series.

The analysis carries through effectively unchanged as before. The net wave-guide field generated by the quadratic interaction of the fermion fields is obtained simply as the sum of the separate wave-guide fields generated by the individual spinor components: there is no contribution to the wave-guide fields from the cross-coupling of spinor fields with different metric indices. The resultant wave-guide fields, including, in particular, the gravitational and electromagnetic far fields, are furthermore real and exhibit the same isotropic tensor forms as in the scalar case.

Finally, the nonlinear eigenvalue equation for the common scalar function $f(r)$ of the spinor fields is identical to the previous nonlinear eigenvalue equation (20) in the scalar case, with $(\kappa^{(c)})^2 = \hat{\omega}^2 - \omega^2$, and with a nonlinear eigenvalue correction consisting as before of a bi-linear product of the function $f(r)$ and the net wave-guide field.

In summary, the computations for the scalar metron solution carry over into the four-spinor case without change for the net wave-guide far fields, while the amplitudes of the four core-mode components (each of which contributes quadratically to the unchanged net wave-guide field) are halved relative to the values for the scalar model.

In the presence of an external magnetic field, the particle spin becomes aligned parallel or anti-parallel to the external field, as in quantum theory, with a resultant net force if the external field is non-homogeneous. However, these considerations, which become relevant mainly in the context of atomic spectra, lie beyond the scope of the present overview.

Missing, finally, in our model of the electron are the weak interactions. The weak charge is represented by the wavenumber component k_5 (Table 1). However, in view of the left-handed chirality of the weak interactions and the finite masses of the associated gauge bosons, the weak forces can clearly not be treated in analogy with the electromagnetic forces (or the strong forces discussed in Section 3.7.3) by simply replacing the electric change k_4 by k_5. Instead, we shall associate the weak interactions later in Section 3.7.4 with interactions with a background wave field that exhibits the exotic properties mentioned.

3.7.2. The neutrino

The metron model of the neutrino depends in detail on the just mentioned representation of the weak interactions later in Section 3.7.4. However, two alternative models can be indicated already here.

In contrast to quantum field theory, in which the breaking of parity symmetry is described by the weak interaction sector of the Standard Model Lagrangian, the metron model attributes these features to an external background wave field. Thus, there is no need to assume (although it can also not be excluded) a breaking of parity symmetry in the metron soliton itself.

Two alternative models of the neutrino can thus be constructed through minor modifications of the electron model. In the first model, we simply replace the electric-charge wavenumber k_4 of the electron by the weak-charge wavenumber k_5, while setting the mass k_0 to zero or a very small number. In the second model, we set also the right-handed core-mode components to zero, in accordance with the quantum theoretical picture that the neutrino itself breaks parity symmetry.

In both cases, we assume that the fibre wavenumber components consist only of the weak-interaction component $k_5^{(\nu)}$ and $k_{11}^{(\nu)} \approx \pm k_5^{(\nu)}$.

3.7.3. The proton-neutron system

The metron picture of the proton-neutron system closely parallels the QFT representation: protons and neutrons are composed of three quarks, which come in two forms: an "up" quark with charge 2/3e and a "down" quark with charge -1/3e. Each quark is characterized by one of three different "colours" (blue, b, green, g and red, r)[6]. The net colour of each three-quark particle is colourless, i.e. each of the three quarks has a different colour, which cancel in the sum. Proton-neutron transformations are furthermore mediated by gauge bosons, that convert an up quark into a down quark, and vice versa.

In the following, we translate these abstract field-operator concepts of QFT into the corresponding metron picture of real existing particles and fields.

The metron model of the proton or neutron consists of three basic core-mode (quark) components, with associated zero-wavenumber wave-guide components. Each quark core-mode component consists of a mirrored pair of four-spinors. The individual metric tensor components of the core modes are assigned to spinor components in accordance with the mapping relations of eq.(24).

The associated wavenumbers of the quarks consist of the components $k_0^{(q)} = m^{(q)} =$ mass, $k_4^{(q)} =$ electric charge, $k_5^{(q)} =$ weak charge, $(k_6^{(q)}, k_7^{(q)}) =$ quark colour-charge vector, and an associated pair of wavenumber components of opposite sign, $\pm k_{11}^{(q)}$, assigned to the two components of a mirrored core-mode pair. The magnitudes of the fibre wavenumber components $\pm k_{11}^{(q)}$ are again chosen such that $(\kappa^{(q)})^2 = -k_L^{(q)} k_{(q)}^L \ll (k_M^{(q)})^2$ for all M. This ensures that $\partial_{\bar{i}} \ll k_M$, as required for the existence of soliton solutions.

The three colour wavenumber vectors, representing the three colour charges blue (b), green (g) and red (r), lie in the k_6, k_7 colour plane (Figure 5). The QFT property of colourless net particles translates into the condition that the vectors form a symmetrical star:

$$\sum_{q=b,g,r} k_6^{(q)} = \sum_{q=b,g,r} k_7^{(q)} = 0, \tag{61}$$

with

$$(k_6^{(b)})^2 + (k_7^{(b)})^2 = (k_6^{(g)})^2 + (k_7^{(g)})^2 = (k_6^{(r)})^2 + (k_7^{(r)})^2 = (k^{(c)})^2, \tag{62}$$

where $k^{(c)}$ represents the magnitude of the strong-force coupling constant.

The star symmetry implies, in particular, that the sum of the strong-interaction wave-guide boson fields generated by the three quarks vanishes: the individual wave-guide fields $h_{06}^{(q)}, h_{07}^{(q)}$ representing the strong force are proportional to the wavenumber product $k_0^{(q)} k_6^{(q)}$, $k_0^{(q)} k_7^{(q)}$, respectively (cf. eq.(50)), so that $\sum_{q=b,g,r} h_{06}^{(q)} = \sum_{q=b,g,r} h_{07}^{(q)} = 0$. Thus, there exist no far fields of the colour force, in agreement with experiment.

---

[6] The index g refers in this section to the colour green, as opposed to the previous reference to wave-guide fields.

For a rigorously spherically symmetric solution, in which all three quarks are located in the same position, the colour forces cancel not only in the far field, but identically[7]. There should therefore exist no inter-nuclear forces, which are normally attributed to the strong forces acting between closely neighbouring nuclei. However, due to the different electromagnetic charges of the quarks, two neighbouring nucleons become polarized, thereby breaking the spherical symmetry and producing a dipole-type near field that is responsible for the inter-nuclear forces.

The representation of the proton-neutron system in terms of real existing quark components explains also the phenomenon of confinement in particle collision processes. At low collision energies, the penetration of the particles into each other's core region is small, and the three quarks of a particle appear as a single particle. However, at higher collision energies with pronounced core penetration, the binding forces of the quarks within a particle become small compared with the forces between the individual quarks of different particles, and the relevant model is that of direct quark-quark interactions.

The nonlinear eigenmode equations for a set of three four-spinor core-mode pairs, with associated field equations for the forced wave-guide fields, follow by straightforward generalization of the scalar model of a single core-mode pair. Thus, eqs. (58)-(60) for a single four-spinor core mode apply in the three-quark case for each of the three four-spinor core modes, and the net wave-guide field is again given simply by the superposition of the wave-guide fields generated by each of the individual core modes.

An additional feature not present in the electron model of a single core-mode pair, however, is the coupling between the three core-mode pairs via their magnetic fields. Thus one needs to distinguish between the net spin 1/2 and (unstable) spin 3/2 configurations.

The magnitudes of the wavenumbers characterizing the various forces in the nuclear system satisfy the inequalities

$$k_0^{(q)} \ll |k_4^{(q)}| \ll k^{(c)} \approx |k_{11}^{(q)}|$$ (63)

As in the electron model, the relevant metron parameters can again be chosen to be consistent with the empirical data.

3.7.4. Weak interactions
In contrast to the metron representation of the strong and electromagnetic forces, which in many respects parallels that of quantum field theory, the metron and quantum-field representations of weak interactions differ significantly. In the Standard Model, the Higgs mechanism plays a central role in explaining the origin of mass, while in the metron model, mass appears naturally as an intrinsic property of the soliton solutions. Furthermore, in the metron model, the left-handed chirality of the weak interactions follows from interactions with a finite-mass, left-hand-polarized background wave field, rather than being defined as a property of the basic Lagrangian. The polarized background wave field, which interacts only with the the left-handed spinor components of the soliton solutions, replaces the finite-mass gauge bosons of the Standard Model.

Figure 11 shows the metron interaction diagram for the example of neutron-proton decay. The background wave field L^- (dotted double-pointed arrow) interacts simultaneously with both the leptons and quarks. Apart from this symmetry, and the fact that L^- represents an external background wave field component rather than a weak-interaction gauge boson W^-, the diagram has the same structure as the corresponding Feynman diagram of the Standard Model.

Whether or not the proposed metron picture is able to reproduce the extensive experimental data on weak interactions remains at this time speculative. The computation of interaction cross

---

[7] The conclusion that the net colour force must vanish also within the particle core has no impact for the trapping of the quark core modes, since the trapping is produced, as in the electron model, by the KSS fields, which, although neglible outside the core region, are dominant and do not cancel within the core.
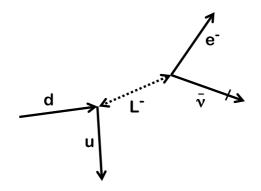
Figure 11. *Metron picture of weak interactions resulting from the coupling of a left-spinor background wave field L^- with left-spinor core-mode components, illustrated for neutron decay. Cross-bars denote complex conjugate fields (in the limit of zero mass, this is identical to the anti-particle).*

sections follows different rules in the metron model, which is concerned with transformations of real solitons, than in quantum field theory, which computes transition probabilities between different states. An additional problem of the proposed metron picture is the experimental instability of the neutron, which contradicts the general stability result cited in Section 3.5.2. The interaction with the background field must enable in this case a "tunnelling" from the quasi-stable neutron soliton to the truly stable proton soliton. However, interactions leading to transitions between two or more soliton solutions, including also particle collision processes in which the solitons penetrate each other's core regions – although well defined mathematically – lie beyond the present overview.

We have also not discussed unstable mesons and the particles of the second and third families. However, the basic picture outlined above – leptons and quarks represented as four-spinor core-mode soliton fields – can be readily applied to the full elementary particle spectrum. Mesons, for example, can be described, in analogy with the Standard Model, as pairs of quarks and anti-quarks of the same colour, while the second and third particle family can be represented as soliton solutions corresponding to the second and third nonlinear eigenmodes of the trapped-mode equations (20) (as demonstrated for the case of the scalar analogue of the Einstein equations in H).

4. Quantum phenomena
The description of elementary particles as soliton solutions endowed with both local corpuscular and large-scale far-field properties represents a first step towards overcoming the wave-particle duality paradoxes of microphysics. The necessary second step is to explain the typical wave-like interference properties observed in particle phenomena at lower atomic-scale energy levels. These result, as mentioned earlier, from interactions of the periodic core mode with other matter.

The particle core modes are generally of too high frequency to directly affect the trajectory of another particle. However, if the core-mode field is scattered off other matter, the interaction of the scattered field with the primary core-mode field of the particle itself generates a low-frequency field through difference-frequency interactions. This is able to modify the particle's trajectory, producing the observed wave-like phenomena. We discuss in the following two cases: the interference patterns of a stream of particles passing through a single or double slit, and the discrete nature of atomic spectra. Similar interpretations can be given for other quantum phenomena, such as Compton scattering, the photo-electric effect and Planck's law.
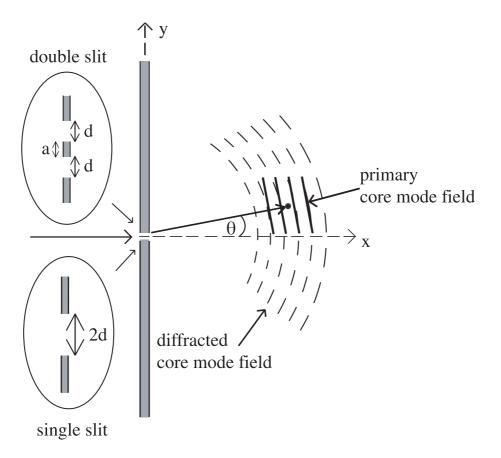
Figure 12. *Interacting primary and diffracted fields of the metron model.*

4.1. Single- and double-slit diffraction

In the metron picture of the single- and double-slit refraction experiment, each particle impinges on some particular position on the detector behind the screen after having passed through the single slit or one of the two slits on a well-defined, but in detail non-measurable, trajectory. The diffraction geometry is shown in Figure 12. The particle source and detector lie in the xy plane, with a screen in the yz plane orthogonal to the x axis at $x = 0$. The slits lie parallel to the z axis. The particles propagate with velocity u parallel to the x-axis, each particle passing through a slit at some random location $\mathbf{x} = (0, y_0, 0)$ at time $t = 0$.

The particle trajectories, after having passed through the diffraction screen, are determined by the force F produced by the interaction between the incident and diffracted core-mode fields. This is given by the negative gradient of the interaction potential V, $F = -\nabla V$, where V is proportional to the integral $< \ldots >$ over the particle core of the product of the (complex conjugate) diffracted secondary field $(\varphi')^*$ and the primary core-mode field φ:

$$V \sim < \Re((\varphi')^*\varphi) > \tag{64}$$

The diffracted secondary wave decays over a range of the order of κ^{-1} (eq.(22). This is large compared with the particle's Compton scale k_0^{-1} (eq.23), but nonetheless finite. The scale κ^{-1} is an important parameter determining the structure of the observed interference pattern (Figures 13, 14).

The interference pattern can be determined by Monte Carlo computations of the paths of individual particles. To compute the particle paths, one needs to: (i) determine the diffracted secondary core-mode field; (ii) evaluate the interaction between the primary and secondary core-
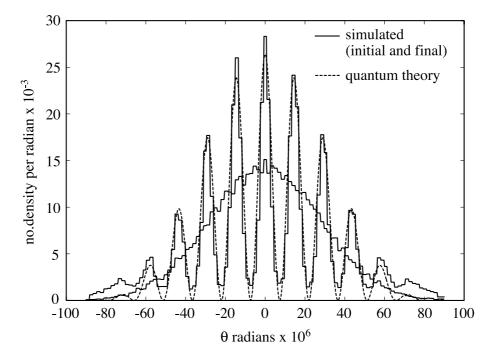
Figure 13. *Quantum theoretical and metron particle distributions for a monochromatic particle beam diffracted at a double slit.*
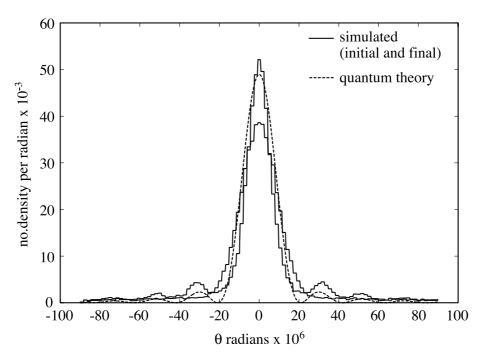

Figure 14. *Quantum theoretical and metron particle distributions for a monochromatic particle beam diffracted at a single slit.*

mode fields and the resultant force F acting on the diffracted particle; and (iii) integrate the trajectory of the diffracted particle underlying the force F.

The first step is similar to the standard computation of the diffracted state function in

quantum theory. The only difference is that, whereas in quantum theory the incident wave is a monochromatic plane wave $\varphi_i \sim \exp[i(kx - \omega t)]$, in the metron model the amplitude of the incident core-mode field of the moving particle is dependent on space and time in the laboratory frame. Thus, both the primary core-mode field and the diffracted field need to be Fourier decomposed.

In the standard quantum theoretical case of an incident plane wave $\exp[i(k\,x - \omega t)]$ and small diffraction angle θ, the diffracted wave φ' at a location $\mathbf{x}' = (x', y' = \theta x', z' = 0)$ and time t' behind the screen is given by

$$\varphi'(x', \theta, t') \sim f_{1,2}(\zeta) \exp i(\mathbf{k}'.\mathbf{x}' - \omega t')(x')^{-1/2} \tag{65}$$

with

$$
\begin{aligned}
f_1(\zeta) &= (2d/\zeta)\sin\zeta \quad \text{(single slit)}, \tag{66}\\
f_2(\zeta) &= (2d/\zeta)\left[\sin\left\{\left(1+\frac{a}{2d}\right)\zeta\right\} - \sin\left\{\frac{a}{2d}\zeta\right\}\right] \quad \text{(double slit)}, \tag{67}
\end{aligned}
$$

where $\zeta = \theta k d$, d is the slit width (double-slit case) or slit half-width (single slit case), a is the double-slit separation, and $\mathbf{k}' = k(\mathbf{x}'/|\mathbf{x}'|)$ is the diffracted wavenumber.

If, instead of a plane wave, the incident field is the core-mode field of a particle travelling through a slit on the path $x = ut, y = y_0, z = 0$, the relations (65)-(67) remain basically unchanged, except that the incident field is multiplied by a modulation factor propagating with the particle velocity u. The diffracted wave field is then similarly modulated, the modulation factor also propagating with group velocity at the speed of the particle, in the slightly modified direction of the diffracted wavenumber. Thus, the incident and diffracted wave field are both transported in a frame moving with the particle.

In addition to propagating at the speed of the particle, the diffracted wave pattern experiences dispersion. This results in a spreading of the wave pattern in the x and z directions and a reduction of the diffracted wave amplitude by an additional factor $1/x'$. The net diffracted field at the position $(\mathbf{x}', t')$ then becomes

$$\varphi'(x', \theta, t') \sim f_{1,2}(\zeta) \exp i(\mathbf{k}'.\mathbf{x}' - \omega t') \exp(-\kappa x')(x')^{-3/2} \tag{68}$$

The probability distribution of the diffracted particles is governed by the tendency of the mean force $\bar{F} = -\nabla \bar{V}$ in the far field to drive the particles into the regions of high $\bar{V} \sim f_{1,2}(\zeta)^2$. The resulting probability distribution resembles, but is not identical to, the quantum theoretical pattern $f_{1,2}(\zeta)^2$.

Figures 13 and 14 show the distributions computed for an ensemble of 40,400 particle trajectories, together with the predictions of quantum theory, for the double- and single-slit cases, respectively. The classical and quantum theoretical distributions agree rather closely for the double-slit case. However, the single-slit distributions, although agreeing in general structure and in the positions of the diffraction maxima, differ in detail. The fit could presumably have been improved by suitable modification of the initial conditions and the parameters of the metron model. A systematic least-square fit was not attempted. However, the point of the exercise is not to reproduce the quantum theoretical predictions, but rather to demonstrate that both quantum theory and a classical model are able to explain, qualitatively, the observed wave-like interference features of particle experiments. Which model yields a better quantitative description of reality must be decided by experiment.

The detailed quantitative verification of de Broglie's 1924 prediction [11] of the wave-like nature of particles in particle diffraction experiments has proved notoriously difficult. Although the positions of the interference maxima predicted by quantum theory were verified in many

experiments, quantitative verification of the complete quantum theoretical diffraction patterns was achieved only after almost seventy years using very low energy neutrons by Zeilinger *et al* [48] and Tschernitz *et al* [45]. In the first of these experiments, excellent agreement with quantum theory was shown for the case of double-slit diffraction, but in the single-slit case, small but statistically significant deviations were found between the predicted and measured diffraction patterns (as well as in a further unpublished experiment mentioned by the authors). Good agreement for the single-slit case was finally achieved by Tschernitz *et al*, but without clearly identifying the origin of the discrepancies in the first experiment. However, the good agreement shown by Zeilinger *et al* in the double-slit case also needs to be revisited: our repeat of the quantum theoretical computations revealed unresolved statistically significant discrepancies (paper in preparation). At this time, the detailed experimental verification or falsification of both the quantal and metron representation of the single- and double-slit diffraction experiments must be regarded as open.

4.2. Atomic spectra

The metron atomic model represents an amalgam of the original Bohr orbital model and the modern wave-dynamics approach of quantum electrodynamics. We consider individual electrons orbiting an atomic nucleus, with associated core-mode fields that are scattered at the atomic nucleus (Figure 15). The scattered core-mode fields ψ satisfy essentially the same field equations

$$(i\gamma^\lambda D_\lambda - \hat{\omega})\psi = F \tag{69}$$

as in QED, where $\hat{\omega} = (-k_l k^l)^{1/2} = (k_0^2 + \kappa^2)^{1/2}$ (eq.(57)) represents the electron mass, to within a small correction term of order $(\kappa/k_0)^2$ (cf. eq.(23)),

$$D_\lambda = \partial_\lambda - ieA_\lambda. \tag{70}$$

is the covariant derivative in the presence of the electromagnetic protential A_λ of the nucleus, and e is the electron charge,.

The only significant difference is that, in contrast to the homogeneous eigenmode equations of QED, eq. (69) includes a source term F representing the forcing by the orbiting electron.

The interaction of the scattered core-mode field with the electron's primary core-mode field produces a low-frequency field which modifies the electron orbit, in the same way as in the particle diffraction case discussed previously. For an arbitrary orbit, the interaction fields and the resultant orbital perturbations are normally small. The electrons therefore gradually drift into orbits of smaller radii through radiative damping. However, for certain discrete orbital parameters, resonances arise in the interacting fields. The perturbations can then no longer be treated as a small stationary response, but grow with time. The solutions stabilize in this case to a stationary state in which the radiative damping of the electron is balanced by the forcing due to the resonant interaction between the electron and the nucleus. The associated net radiative damping of the complete coupled electron-nucleus system vanishes.

For the case of circular orbits, the resonant interaction conditions for the primary and scattered core modes are found to be identical to lowest order to the QED eigenmode conditions, while the associated resonant orbital conditions correspond to Bohr's original orbital conditions (H). Detailed computations at the extremely high level of accuracy as achieved in the QED computations of the hydrogen atom, for example, have still to be performed. Although it may appear intrinsically unlikely that the same results as QED, based on an array of higher order corrections, including renormalization, can be achieved with an alternative classical theory, it is perhaps encouraging that Barut [3] has claimed that a non-second-quantized theory, without invoking renormalization, yields still higher agreement with experiment than QED.
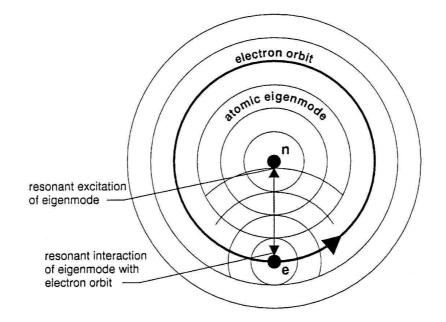
Figure 15. *Metron model of electron orbiting an atomic nucleus. The low-frequency field produced by the difference interaction between the primary core-mode field of the electron and the secondary core-mode field scattered at the atomic nucleus modifies the electron orbit. Resonance between the electron orbit and the difference-frequency field produces trapping of the electron in discrete orbits in accordance with Bohr's original discrete-orbit model. The resonant scattered core-mode fields correspond to the QED eigenmodes (reproduced from [27]).*

The attraction of the present ansatz is that it explains the discrete nature of atomic spectra as a resonance phenomenon of real existing particles supporting real continuous fields, without the need to switch pictures between fields and particles. Thus the photo-electric effect, for example, in which discrete electron particles are released from atomic states through incident electromagnetic radiation is readily explained without rejecting the concept of discrete localized particles in the description of the atomic states that release the observed discrete particles.

5. Summary

As precondition for the development of a classical unified theory, we have shown first that Bell's theorem, which has been widely interpreted as implying that classical theories are incapable of explaining the phenomenon of entanglement observed in microphysical phenomena, does not apply to classical models satisfying time-reversal symmetry. Entanglement is a universal property of all theories exhibiting time-reversal symmetry, whether classical or quantal. It follows directly from the relativistic implications of Newton's third law *actio = reactio*.

The basic concept of our classical model is very simple: the wave-particle duality paradoxes that led to the creation of quantum theory and its later special relativistic generalization, quantum field theory, can be explained in terms of the periodic soliton solutions of the Einstein vacuum equations $E_{LM} = 0$ in a twelve dimensional space. The finite extent and periodicity of the solitons provide a straightforward classical interpretation in terms of real existing objects of the various abstract features of quantum theory and quantum field theory.

The metron core modes correspond in many respects to the state function of quantum theory. From the metron viewpoint, the success of quantum theory, for example in atomic physics, is

attributed to the theory reproducing the field properties of the core mode, while its conceptual difficulties arise from its inability to capture also the associated corpuscular features. This is elevated to a quantum theoretical theorem in Heisenberg's uncertainty principle. This is not in conflict with the metron model. Quantum theory is regarded as a theory of incomplete information. The uncertainty principle is justified empirically for both quantum theory and the metron model by the usual argument that initially limited information cannot be augmented subsequently by measurements using some (similarly imperfectly known) system that modifies the state to be measured.

Other basic quantal concepts, such as Fermi-Dirac and Bose-Einstein statistics, or vacuum state fluctuations, can be similarly translated in the metron model into classical processes involving real existing objects – avoiding thereby also divergent integrals and the need for renormalization.

In contrast to the mathematical formulation of quantum field theory based on the Standard Model Lagrangian and its symmetries, we have made no reference in the metron model as summarized here to the Einstein-Hilbert Lagrangian or the invariance of the Einstein equations with respect to coordinate transformations. We have simply exploited the fact that the Einstein equations are nonlinear, and then applied standard perturbation theory to study the interactions between the periodic core modes and higher-order components of the soliton solutions. The symmetries of the Standard Model correspond in the metron picture to the invariance with respect to translations in the fibre coordinates (i.e. phase shifts) and, in the case of strong interactions, the geometrical symmetries of the wavenumber configurations. Whether the Higgs mechanism and the internal breaking of parity symmetry can be replaced by the proposed simpler interaction with an external left-polarized high-mass background wave field remains to be investigated. In principle, however, the mathematics of the metron model is basically simple and can be summarized in terms of elementary interaction diagrams. This applies both to the structure of elementary particles and the explanation of the wave-particle duality paradoxes observed at lower energies.

Our overview of a proposed classical interpretation of elementary particles and quantum phenomena is necessarily of wide sweep and leaves open many questions. However, an alternative to a technically highly successful theory that has evolved over nearly a century can clearly not be developed in only a few papers. A comparison of the present presentation with its predecessors [23] - [28] reveals that, although the basic concepts have withstood the test of time, the metron model is still very much in flux. Nevertheless, a number of open questions listed in the conclusions of [26], such as the stability and uniqueness of the metron solitons and the origin of the basic physical constants, have now been successfully addressed.

Our motivation has not been to explain experimental results in conflict with current physical theory - often regarded as the litmus test of a new paradigm - but rather to offer an alternative view of physical reality that unifies the general relativistic theory of gravity with our understanding of elementary particles and quantum phenomena, avoiding in the process the conceptual difficulties of quantum field theory. Despite the undisputed successes of quantum field theory, its underlying conceptual fuzzines and its incompatability with general relativity have concerned not only Einstein, but many leading physicists. We believe that the path we have explored offers a new perspective for overcoming these inconsistencies and developing a conceptually better founded unified theory.

comments.

References

[1] H. Abraham. *Ann.d.Physik*, 10:105, 1903.

[2] A. Aspect, P. Grangier, and G. Roge. Experimental Realization of Einstein-Podolsky-Rosen-Bohm Gedankenexperiment: A New Violation of Bell's Inequality. *Phys. Rev. Letters*, 49:91–94, 1982.

[3] A. O. Barut. Quantum-electrodynamics based on self-energy. *Physica Scripta*, 21:18–21, 1988.

[4] G. Basini, S. Capozziello, and G. Longo. The Einstein-Podolsky-Rosen Effect: Paradox of Gate? *General Relativity and Gravitation*, 35:189–200, 2003.

[5] J. S. Bell. On the Einstein-Podolsky-Rosen paradox. *Physics*, 1:195–200, 1964.

[6] D. Bohm. A suggested interpretation of the quantum theory in terms of "hidden variables", Parts 1 and 3. *Phys.Rev.*, 85:165–179 and 180–193, 1952.

[7] F. Cianfrani and G. Montani. Towards loop quantum gravity without the time gauge. *Phys.Rev.Lett*, 102:91301–91305, 2009.

[8] O. Costa de Beauregard. Time symmetry and the interpretation of quantum mechanics. *Foundations of Physics*, 6:539–559, 1976.

[9] J. G. Cramer. The transactional interpretation of quantum mechanics. *Rev. Mod. Phys.*, 58:647–687, 1986.

[10] W. C. Davidon. *Nuovo Cimento*, B 36:34, 1976.

[11] L. de Broglie. Recherches sur la thorie des quanta (researches on the quantum theory), thesis, paris 1924. *Ann. de Physique*, 3:22, 1925.

[12] L. de Broglie. *Compt. Rend. Acad. Sci.,Paris*, 183:447–448, 1926.

[13] L. de Broglie. *Nature*, 118:441–442, 1926.

[14] A. Einstein. Zum gegenwärtigen Stand des Strahlungsproblems. *Phys.Z.*, 10:185–193, 1909.

[15] A. Einstein. Quantentheorie der strahlung. *Phys.Z*, 18:121–128, 1917.

[16] A. Einstein, B. Podolsky, and N. Rosen. Can quantum-theoretical description of physical reality be considered complete? *Phys. Rev.*, 47:777–780, 1935.

[17] A.D. Fokker. An invariant variation principle for the motion of many electrical mass particles. *Z.Phys*, 58:386–393, 1929.

[18] S. J. Freedman and J. F. Clauser. Experimental test of local hidden-variable theories. *Phys. Rev. Letters*, 28:938–941, 1972.

[19] J. Frenkel. Zur Elektrodynamik punktörmiger Elektronen. *Z.Phys.*, 32:518–534, 1925.

[20] L. Gilder. *The Age of Entanglement: When Quantum Physics was Reborn*. Knopf, 2008.

[21] M. Göckeler and T. Schückeler. In *Differential Geometry, Gauge Theories and Gravity*. Camb. Univ. Press, Cambridge, 1987.

[22] B.R. Greene. *The Elegant Universe*. Vintage, London, 2000.

[23] K. Hasselmann. The metron model: Elements of a unified deterministic theory of fields and particles. part 1: The metron concept. *Physics Essays*, 9:311 – 325, 1996.

[24] K. Hasselmann. The metron model: Elements of a unified deterministic theory of fields and particles. part 2: The maxwell dirac-einstein system. *Physics Essays*, 9:460–475, 1996.

[25] K. Hasselmann. The metron model: Elements of a unified deterministic theory of fields and particles. part 3: Quantum phenomena. *Physics Essays*, 10:64 – 86, 1997.

[26] K. Hasselmann. The metron model: Elements of a unified deterministic theory of fields and particles. part 4: The standard model. *Physics Essays*, 10:269 – 286, 1997.

[27] K. Hasselmann. The metron model. towards a unified deterministic theory of fields and particles. In A.K. Richter, editor, *Understanding Physics*, pages 154–186, Copernicus Gesellschaft e.V. Kathlenburg-Lindau, Germany, 1998.

[28] K. Hasselmann and S. Hasselmann. The metron model. a unified deterministic theory of fields and particles - a progress report. In *Proc. 5th Intern.Conf., Symmetry in Nonlinear Mathematical Physics*, pages 788–795, Kyiv, 23-29 June 2004.

[29] P.R. Holland. *The Quantum Theory of Motion. An Account of the de Broglie-Bohm Causal Interpretation of Quantum Mechanics*. Cambridge Univ. Press, 1993.

[30] F. Hoyle and J.V. Narlikar. A new theory of gravitation. *Proc. Roy. Soc. A*, 282:191–207, 1964.

[31] C.J. Isham. *Modern Differential Geometry for Physicists*. World Scientific, 1999.

[32] T. Kaluza. Zum unitätsproblem der physik. *Sitzungsber.d.Preuss.Akad.d.Wiss*, pages 966–972, 1921.

[33] O. Klein. Quantentheorie und fünfdimensionale relativitätstheorie. *Z.Phys.*, 37:895–906, 1926.

[34] W. Kundt. Fundamental physics. *Foundations of Physics*, 37:1317–1369, 2007.

[35] H.A. Lorentz. republished in collected papers. volume II, page 281 and 343. 1892.

[36] H.A. Lorentz. The theory of electrons. Leizig, 1909.

[37] C.W. Misner, K.S.Thorne, and J.A.Wheeler. *Gravitation*. W.H.Freeman & Co., New York, 1973.

[38] R. Penrose. *The Road to Reality*. Vintage Books, New Yord, 2007.

[39] J. Polchinksi. *String Theory*. Camb.Univ.Press, Cambridge, 1998.

[40] W.M. Ritz. Recherches critiques sur l'électrodynamique géneral. *Ann. Chim.Phys.*, 13:145–275, 1908.

[41] E Schrödinger and M. Born. Discussion of probability relations between separated systems. *Math. Proc. Cambr. Phil. Soc.*, 31:555–563, 1935.

[42] L. Smolin. *Three Roads to Quantum Gravity*. Phoenix, Phoenix, 2001.

[43] N. Steenrod. *The Topology of Fibre Bundels*. Princeton University Press, Princeton, 1951.

[44] H. Tetrode. Über den Wirkungszusammenhang der Welt. Eine Erweiterung der klassischen Dynamik. *Zeitschrift für Physik*, 10:317–328, 1922.

[45] M. Tschernitz, R. Gähler, W. Mampe, B. Schillinger, and A. Zeilinger. Precision measurements of single slit diffraction with very cold neutrons. *Phys.Lett.*, A 164:365–368, 1992.

[46] J.A. Wheeler and R.P. Feynman. Interaction with the absorber as the mechanism of radiation. *Rev.Mod.Phys.*, 17:157–181, 1945.

[47] J.A. Wheeler and R.P. Feynman. Classical electrodynamics in terms of direct particle interactions. *Rev.Mod.Phys.*, 21:425–433, 1949.

[48] A. Zeilinger, R. Gähler, C.G. Shull, W. Treimer, and W. Mampe. Single- and doppel-slit diffraction of neutrons. *Rev.Mod.Phys.*, 60:1067–1073, 1988.

[49] A. Zeilinger, G. Weihs, T. Jennewein, and M. Aspelmeyer. Happy centenary, photon. *Nature*, 433:230–238, 2005.